



Heat Capacity of Fe_3O_4 (Magnetite) (Heat Capacity Option)

<http://education.qdusa.com/experiments.html>

Prof. Stephen Tsui and Silvia Sherman
California State University San Marcos

Prof. Richard Averitt
University of California, San Diego

In this Educational Module, students will measure the heat capacity of Fe_3O_4 , more commonly known as magnetite. This material undergoes a structural phase transition that can be observed in both its electrical transport and magnetic properties. The primary emphasis will be to characterize this "Verwey transition", the underlying physics of which continues to be studied to this day.

Introduction:

Magnetite (Fe_3O_4) is a naturally occurring mineral that historically has been called "lodestone". Lodestone was sought throughout antiquity due to its attractive ferromagnetic properties [1]. Today, magnetite is used in several industrial applications that include inks and cosmetics [2]. It has even been discovered that magnetotactic bacteria are capable of producing this material [3]. In 1939, Evert J. W. Verwey investigated the resistivity vs. temperature behavior of Fe_3O_4 and identified a transition at ~125K whereby the resistivity increased by two orders of magnitude (Fig. 1) [4, 5]. He attributed this behavior to a charge ordering transition, where said ordering removed the necessary fluctuations required for metallic conduction, and his name has been associated with this phenomenon ever since.

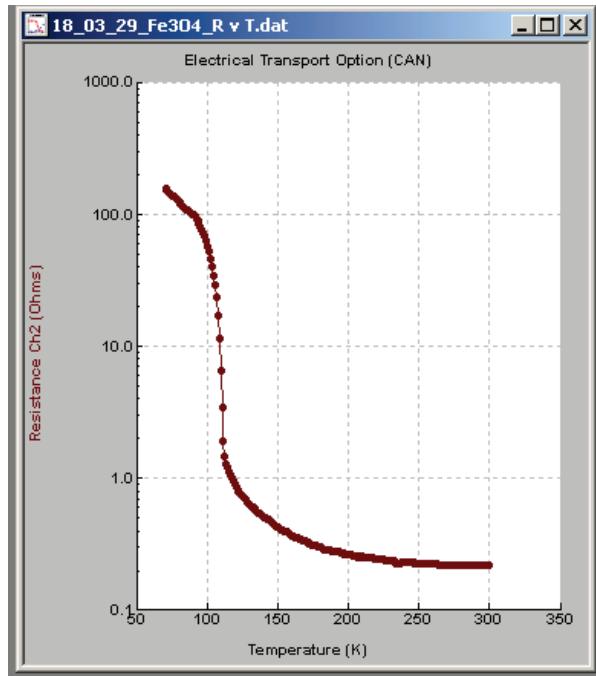


Figure 1: The Verwey transition as shown in a plot of resistance vs. temperature, as measured in a VersaLab with the Electrical Transport Option (ETO).

In addition to being studied electrically, it has also been reported that a change in the magnetic anisotropy – the directional dependence of a material's magnetic properties – due to the change in the crystalline symmetry can be observed at the Verwey temperature [6]. As a result, the Verwey transition can also be observed through a magnetic measurement.

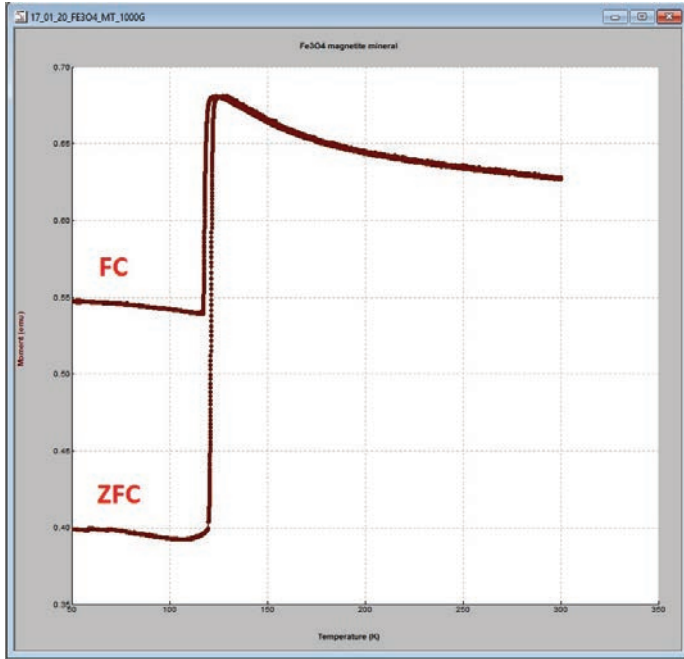


Figure 2: The Verwey transition as demonstrated by plots of zero-field-cooled (ZFC) and field-cooled (FC) magnetic moment vs. temperature measured using a VersaLab with the Vibrating Sample Magnetometer (VSM) Option.

Studies on the unique physical properties of Fe_3O_4 continued for decades after its initial characterization. Recent work has probed the atomic structure of Fe_3O_4 via powder X-ray diffraction and Mössbauer spectroscopy [7]. From this work a structural phase transition, from an inverse to normal spinel (Fig. 3), was proposed to explain the behavior observed upon cooling through the Verwey transition. However, this structural transition does not completely describe the presence of charge ordering, and contemporaneous studies suggest that the formation of a three-site Fe trimeron sublattice is responsible for the electronic ordering [8]. As such, the subtle and interesting underlying physics describing the microscopic details of the transition continue to be studied to this day.

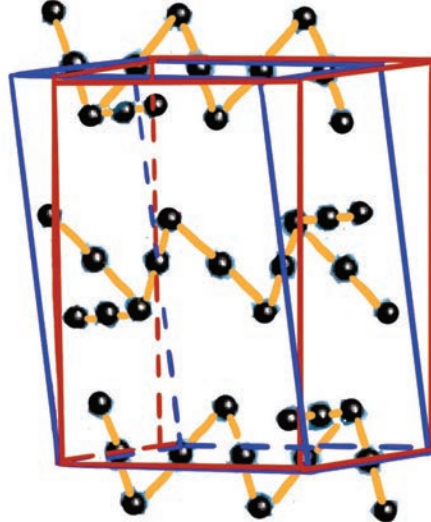


Figure 3: Sketch showing the Fe sublattice and the structural phase transition between the high temperature cubic inverse spinel in red and the low temperature monoclinic spinel in blue [7, 8].

Student Learning Outcomes:

- Students will gain experience with small sample handling.
- Students will learn how to perform a heat capacity measurement.
- Students will observe a first order phase transition and experience the technical nuances with such a measurement.
- Students will apply foundational knowledge of relevant solid state physics to heat capacity characterization.

Safety Information:

Before attempting to perform any parts of this student experiment, please read the entire contents of: this Educational Module, the VersaLab User's Manual (1201-300), and Heat Capacity Option User's Manual (1085-150), and observe all instructions, warnings and cautions. These are provided to help you understand how to safely and properly use the equipment, perform the experiments and reach the best student learning outcomes.

Quantum Design Inc. disclaims any liability for damage to the system or injury resulting from misuse, improper operation of the system and the information contained in this Educational Module.

The following Safety warnings apply to this Educational Module:

WARNING!

Always use Personal Protective Equipment (PPE) during every step of the sample preparation. Failure to do so might cause bodily harm.



CRUSHING HAZARD!



Before using the die and hydraulic press, please read the entire contents of the User's Manual specific to that equipment, and observe all instructions, warnings and cautions. Failure to do so might cause bodily harm and or death.

Measurement Background:

The heat capacity [J/K] characterizes the increase in the internal energy of a system for a given temperature increase. Consider the first law of thermodynamics: $dU = dQ + dW$, where dU is the change in energy when either work (dW) is performed or heat (dQ) is added to the system. This expression can also be written as $dU = TdS - PdV$ where the notation follows standard conventions. The heat capacity is defined as $C = dQ/dT$ which, for constant volume, is $C_V = dU/dT = T(dS/dT)$ [9,10]. Heat capacity is an extensive property (i.e. it depends on the quantity of material) with units of J/K . It is often helpful to express it instead as an intensive quantity. Two common intensive descriptions are the mass heat capacity (often called the mass specific heat) with units $J/(kg\ K)$ and the molar heat capacity (often called the molar specific heat) with units of $J/(mol\ K)$. The same symbol c_V is typically used for either specific heat quantity, so care must be taken to specify the units. For solid-state measurements, it is usually the specific heat at constant pressure c_p that is measured. The connection between c_V and c_p is $c_p - c_V = \kappa\alpha^2VT$ where α [$1/K$] is the linear coefficient of expansion, κ [$m\cdot s^2/kg$] is the compressibility, and V [m^3/kg] is the specific volume. For the purposes of this module, the distinction is not critical, however.

Heat capacity measurements provide fundamental insight into the properties of a material. Recall the classical result of Dulong-Petit for the molar heat capacity of a solid: $c = 3R = 24.9 \text{ J/(mol K)}$ where $R = 8.31 \text{ J/(mol K)}$ is the ideal gas constant. This provides reasonable agreement with the room temperature measurement of many solids (e.g. Aluminum (24.2), Fe (25.1)). However, strong deviations of materials such as diamond (6.1) and, more importantly, the temperature dependence of the heat capacity necessitates the use of quantum mechanics to obtain a more complete understanding. In Einstein's theory, the solid is treated as a group of harmonic oscillators with a single characteristic vibrational frequency ω [11]. This approach was able to provide a basic understanding of the decrease in the heat capacity with temperature. The data for diamond with Einstein's fit is shown in Fig. 4. In this plot the units are cal/(mol K) which can be converted to J/(mol K) by multiplying by 4.184 J/cal. For diamond, the Einstein temperature is given by $T_E = \hbar\omega/k_b = 1320 \text{ K}$ indicating the approximate temperature at which the heat capacity reaches the classical Dulong-Petit value. The deviations at low temperature between experiment and theory in Fig. 4 are not due to instrument error; instead a better fit is obtained with the Debye model which essentially quantizes acoustic waves. Amongst other things, the Debye model correctly predicts the T^3 dependence of the heat capacity of insulators at low temperatures [10].

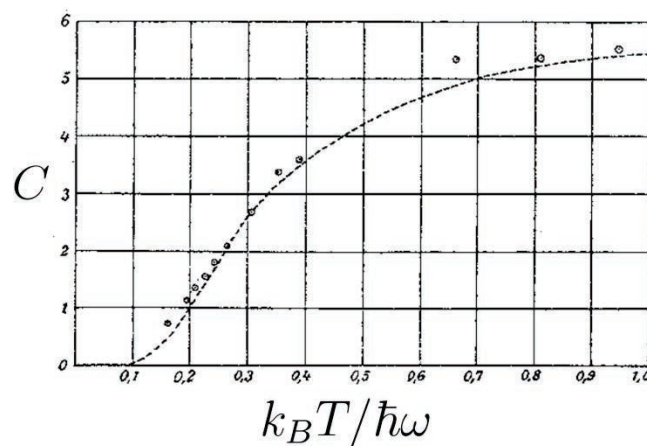


Figure 4: Comparison of Einstein model (dashed line) to experiment (circles) for the molar specific heat of diamond from [11].

Importantly, other degrees of freedom in solids also contribute to heat capacity. For example, in metals the specific heat exhibits a linear dependence on temperature $c = \gamma T$ arising from the free electrons in the material (γ is known as the Sommerfeld coefficient). This was first correctly obtained in free electron (or Sommerfeld) theory using Fermi-Dirac statistics for the electrons [10]. Of course, $c = \gamma T$ is just for the electrons, and the lattice must also be included. At low temperatures, $c \approx \gamma T + \beta T^3$ where the linear term is for the electron contribution and

the cubic term is due to the lattice vibrations. At high temperatures, the lattice contribution will dominate, but the electron contribution becomes important in metals at low temperatures.

In contemporary condensed matter physics, the fact that heat capacity measurements reveal interactions between various degrees of freedom is extremely important. As one example, consider heavy-Fermion (HF) materials. As the name implies, in these materials (below a cross-over temperature), the electrons (really quasiparticles – *i.e.* dressed electrons) become extremely heavy. In some HF materials the quasiparticles exhibit an effective mass approaching 1000 times the mass of a free electron! This arises from interactions of the conduction electrons with localized f-moments in these materials. Importantly, the onset of HF phenomena appears in heat capacity measurements. This is because the heat capacity is proportional to the density of states at the Fermi level, which in turn is related to the effective mass [12,13].

Heavy Fermions are but one (fairly exotic) example. More generally, heat capacity measurements are sensitive to phase transitions. This includes magnetic ordering, structural transitions, ferroelectric polarization, and superconductivity. This applies to both first order and second order phase transitions. In the case of a first order transition, a discontinuity appears in the entropy which in turn leads to a divergence in the specific heat since $c_v = T(dS/dT)$. This singularity is the latent heat L [J/kg] and is the increase in the internal energy needed to drive the phase transition [14].

In the case of a second order (or continuous) phase transition, a kink appears in the entropy S, leading to a discontinuity in the specific heat. The importance of this can be understood from considering thermodynamic potentials. For example, for the Helmholtz free energy we have $F = U - TS$. From this we can see that the entropy is the driving “force” for a phase transition. At low temperature (below the phase transition temperature T_c), the entropy is not too important, and F can be minimized by having U minimized. This leads to ordering (*e.g.* of spins in a magnet). However, with increasing temperature the entropy becomes increasingly important, and minimizing F benefits from increased S corresponding to increasing disorder. In fact, the total entropy associated with the ordering can be determined from:

$$S = \int_0^{T_c} \frac{1}{T} c_p(T) dT \quad (\text{Eqn. 1})$$

In determining the entropy associated with ordering, it is important to exclude other contributions such as the lattice specific heat. An insightful description of second order (and also first order) phase transitions is Landau’s mean field theory which provides a description in terms of an order parameter [15]. However, while

providing considerable insight and a general framework for phase transitions, this theory does not include fluctuations, which affect the thermodynamic response and lead to interesting phenomena such as critical behavior in phase transitions [15,16]. A detailed description of critical phenomena, ordering and broken symmetry, etc., can be found in the references. Suffice to say, heat capacity measurements are a primary means to study these fundamentally important effects in solids.

The next question we must address is how are heat capacity measurements performed? The basic idea is to heat the sample in a precise manner to add a known amount of energy and measure the corresponding temperature change. In the VersaLab heat capacity option, this is accomplished by applying a known amount of heat at constant power for a fixed amount of time followed by a cooling period while measuring the temperature as a function of time. This heating/cooling process is depicted in Fig. 5. An appropriate model (discussed below and in Chapter 4 of the heat capacity option user's manual) is used to fit the time dependence of the temperature change which in turn can be leveraged to determine the heat capacity.

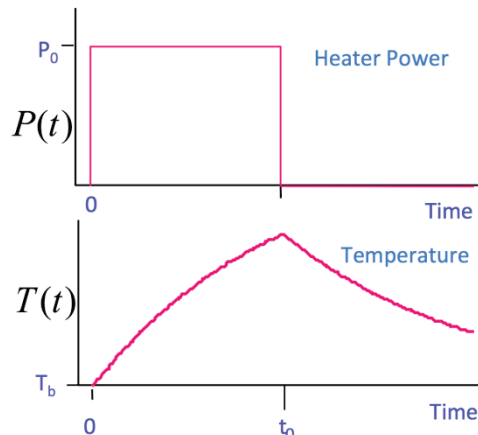


Figure 5: Heat capacity measurement approach.

For accurate measurements, the heat capacity hardware must be designed to have a low thermal mass and appropriate thermal conductance and thermal isolation. Fig. 6a gives a schematic depiction of the hardware, while Fig. 6b is a picture of the heat capacity puck used for the VersaLab.

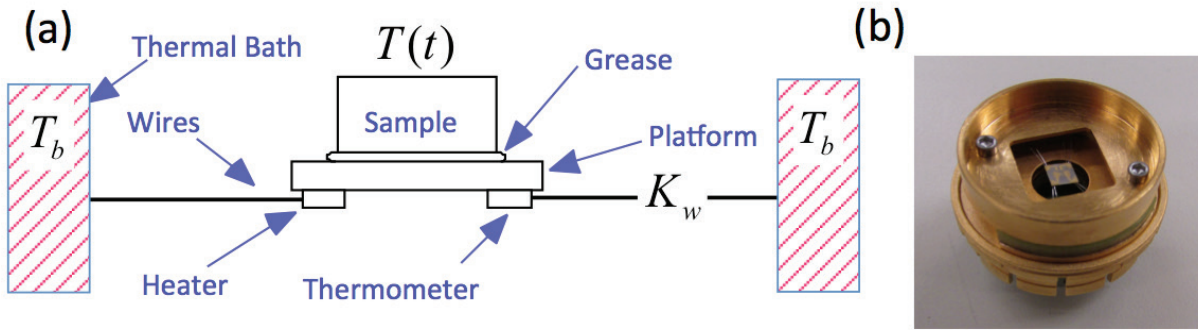


Figure 6: (a) Schematic of heat capacity hardware. (b) Actual heat capacity puck.

As shown in Fig. 6, a platform heater and platform thermometer are attached to the bottom side of the sapphire (Al_2O_3) sample platform. Small wires provide the electrical connection to the platform heater and platform thermometer and also provide the thermal connection and structural support for the platform. The sample is mounted to the platform by using a thin layer of grease, which provides the required thermal contact to the platform.

The integrated vacuum system in the cryostat provides a sufficient vacuum so that the thermal conductance between the sample platform and the thermal bath (puck) is dominated by the conductance of the wires. This gives a reproducible heat link to the bath with a corresponding time constant large enough to allow both the platform and sample to achieve sufficient thermal equilibrium during the measurement.

The VersaLab measures heat capacity curves like that shown in Fig. 5 (*i.e.* the change in temperature versus time), and the data is fitted in MultiVu using one of several models. To give a feel for this, the 1-tau model that fits the data using a single time constant is described here. The details of the 2-tau model (which accurately accounts for finite thermal conductance between the sample and the platform) are described in section 4.3 of the Heat Capacity Option User's Manual. The 1-tau model describes the flow of power into and out of the sample:

$$C_{total} \frac{dT(t)}{dt} = P(t) - K_w(T(t) - T_b) \quad (\text{Eqn. 2})$$

where C_{total} is the total heat capacity, $P(t)$ is the applied power, K_w is the thermal conductance of the wires, $T(t)$ is the time-dependent temperature, and T_b is the bath temperature. For $P(t)$ (see Fig. 5) we have $P(t) = P_0$ ($0 \leq t \leq t_0$) and $P(t) = 0$ ($t > t_0$). With the initial conditions, $T_{on}(0) = T_b$ and $T_{on}(t_0) = T_{off}(t_0)$, Eqn. 2 can be solved yielding:

$$T(t) = \begin{cases} \frac{P_0\tau(1-e^{-\frac{t}{\tau}})}{C_{total}} + T_b & (0 \leq t \leq t_0) \\ \frac{P_0\tau(1-e^{-\frac{t}{\tau}})e^{-(t-t_0)/\tau}}{C_{total}} + T_b & (0 > t_0) \end{cases} \quad (\text{Eqn. 3})$$

where $\tau = C_{total}/K_w$ is the thermal time constant. MultiVu uses a least-squares method to obtain the fit of the data from which the heat capacity is extracted. Performing these thermal time constant measurements at a series of temperatures allows for the determination of the heat capacity as a function of temperature.

It is important to note that C_{total} is the total heat capacity of the platform, the grease, and the sample of interest. Thus, several measurements are actually required to obtain C_p of the sample. First, the puck must be calibrated. That is, a measurement must be performed without the grease or the sample. This procedure needs to be performed for each newly-built puck to determine the thermometry calibration and K_w . The data for this calibration is saved in a ".cal" file for reference with the subsequent measurements. For each new sample to be measured, an addenda must first be obtained. This is essentially a measurement of the heat capacity of the grease and the sample platform **without** the sample. These addenda are also saved in the calibration file. Finally, the sample/grease/sample platform heat capacity is measured. In this way, it is possible to obtain C_p of the sample of interest.

While this approach for measuring the heat capacity enables measurements over a wide temperature range, it could easily miss features in the specific heat associated with first or second order phase transitions if, for example, the selected number of temperature points are too sparse. This is because the heat capacity associated with phase transitions can be quite narrow (this is particularly true for first order transitions). Thus, an alternative approach to measure (or search for) the phase transition must be utilized.

In this study, we will utilize the slope analysis method of relaxation curves. If both sides of Eqn. 2 are divided by $dT(t)/dt$, one obtains:

$$C_{total} = \frac{P(t) - K_w(T(t) - T_b)}{dT/dt} \quad (\text{Eqn. 4})$$

This provides an operational approach to obtain the heat capacity as a function of temperature from a single curve such as that shown in Fig. 5. Over each small time interval the slope is calculated, thereby providing a means to obtain C_{total} at various points on the curve. In the case of a first order phase transition, there should be a distinct decrease in the slope at the transition temperature. This intuitively makes sense, since the latent heat requires the addition of energy to

the sample without a temperature increase. Further, as first order transitions exhibit hysteresis, the warming and cooling curves will have different kinks in the slopes. Section 4.3 of the heat capacity user manual presents additional details while section 4.6 provides examples of single slope analysis of a first order phase transition in Figs. 4-6 and 4-7. It is strongly advised that chapters 1-4 of the heat capacity user's manual is read prior to performing these measurements.

Materials List:

Sample Preparation
Magnetite Sample or Powder
Balance
Weighing Paper or Weighing Boats
Apiezon N Grease
Microscope
Tweezers

Fe₃O₄ Sample Preparation:

If your magnetite sample is in a naturally occurring rock form, wear the proper personal protective equipment (PPE) and break off a small piece of magnetite (Fig. 7). One recommended procedure is to place the mineral in a bag and carefully strike it with a hammer. Be sure to measure the mass of your sample.



Figure 7: Magnetite with pieces broken off.

If you are using commercial Fe₃O₄ powder, you should press the powder into a pellet using a die and hydraulic press.

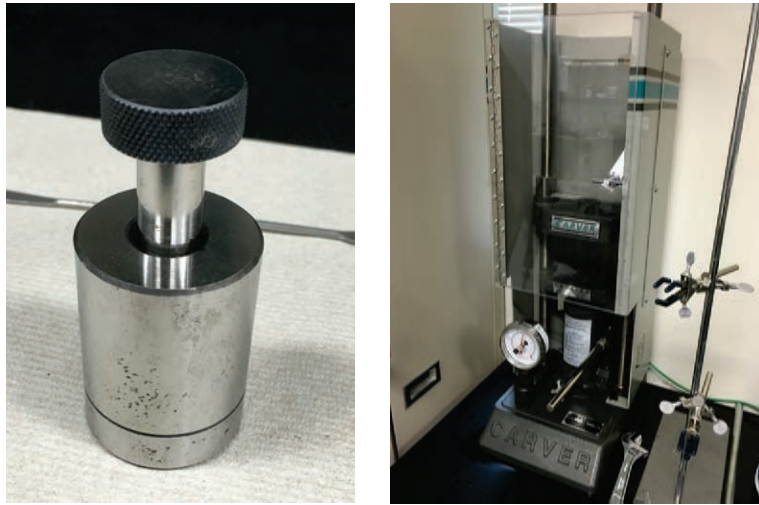


Figure 8: 13 mm die set (left) and hydraulic press (right).

Fill a small amount of power into the die. Applying 13,000 pounds of with the hydraulic press is sufficient to yield a pellet. It should be fairly easy to break off a small piece of sample by poking at it with a stick or tweezers in order to fit into the heat capacity puck. However, do not do this yet! The puck must be measured without a sample first in order to properly obtain the heat capacity.

Experimental Instructions:

In this section, we provide guidance on preparing and measuring the heat capacity.

Several items are needed for this experiment, which includes:

- Apiezon N grease. Note that the specific heat of N grease is strongly temperature dependent above 200K, while H grease has been known to pop off the sample platform at low temperatures.
 - A microscope to facilitate the application of the grease and sample
 - A precision scale with 0.1 mg or better resolution.
 - Weigh boats or wax paper for handling the sample.
- a.) Prior to preparing for the sample measurement, the heat capacity module should be installed, and the option software activated. In addition, make certain that the sample mounting station and its small pump are in an easy to access location.

b.) Locate the heat capacity puck and thermal radiation shield.



Figure 9: Heat capacity puck and shield

- c.) Verify that the serial number of the puck has a corresponding calibration file in MultiVu. This can be checked in the heat capacity control center (see section 4.4. of the user manual). Clicking on the "files" tab will enable identification of the calibration file. In the following, we will assume that the puck in use has been properly calibrated. If not, the procedure in Chapter 5 of the heat capacity user's manual must be followed.
- d.) The next step is to prepare the puck for the addenda measurement. This requires placing a small amount of N grease on the puck area where the sample will be placed. For this, the sample mounting station is utilized. This is to stabilize the puck while working with it, since the sample platform is very fragile, and it is easy to break the wires! Fig. 10 shows the heat capacity puck inserted. With the lever arm in the open position as shown, the vacuum is not on. Upon closing (see Fig. 11) the vacuum line will be activated (make sure the pump is on!) which will gently pull the sample platform into place, thereby stabilizing it for grease application.

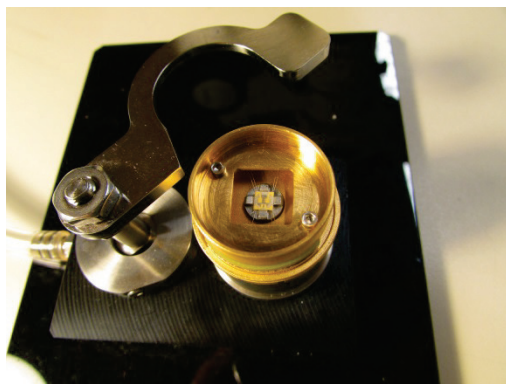


Figure 10: Heat capacity puck in the mounting station.

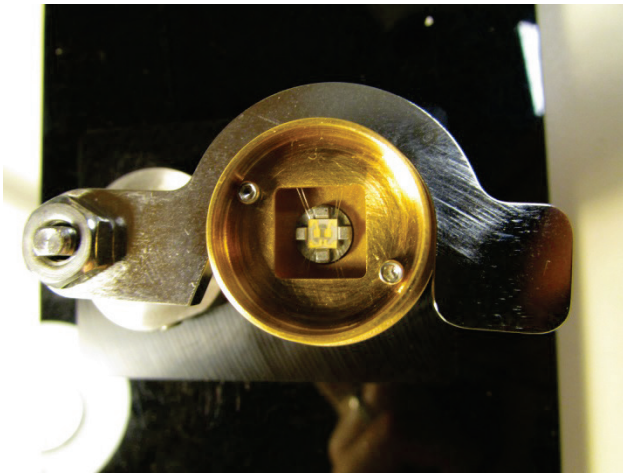


Figure 11: With the lever closed, the platform is stabilized.

e.) The next step is to place the N grease on the platform, being careful to not touch the wires. There are two reasons for this. First, the wires could break. Secondly, any grease that gets on the wires will change the thermal conductance, which could invalidate the calibration. Fig. 12 shows the grease being placed on the sample stage, and Fig. 13 shows a close up of the sample stage after the grease application.

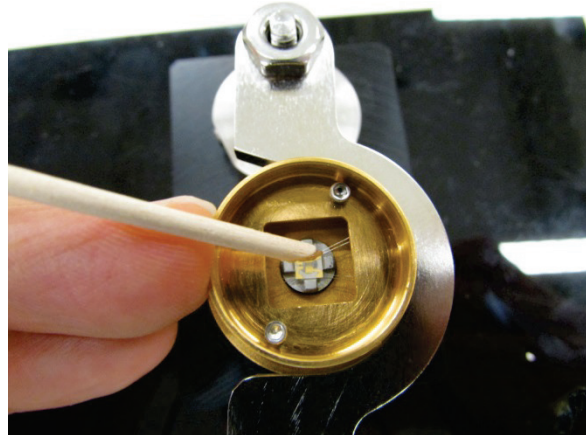


Figure 12: N grease application to sample platform

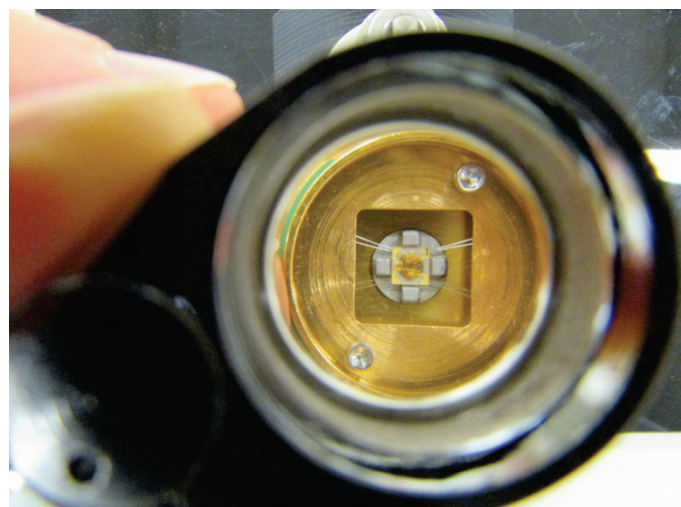


Figure 13: Sample platform with grease applied.

- f.) The next step is to perform the addenda measurement. First, ensure the thermal radiation shield is firmly fastened to the puck as shown in Fig. 14.

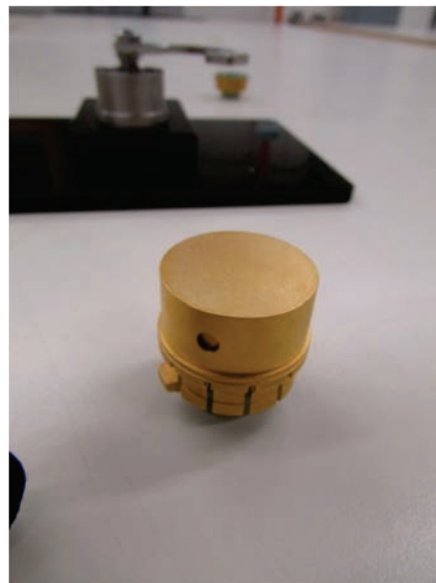


Figure 14: Heat capacity puck ready for addenda measurement

- g.) The puck can now be loaded into the VersaLab (Fig. 15), and the VersaLab chamber sealed using the cap with the attached baffle set (Fig. 16).



Figure 15: Loading the puck into the VersaLab.

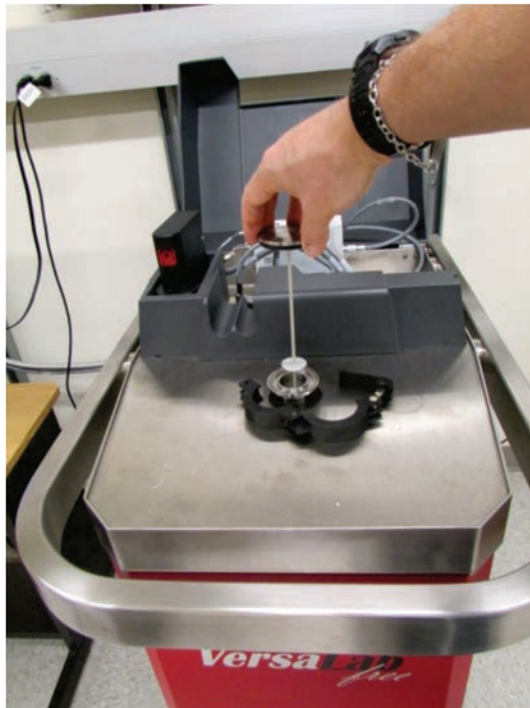


Figure 16: Sealing the VersaLab for the addenda measurement using the cap with thermal baffles attached.

- h.) In the heat capacity control center (again, see section 4.4 of the user's manual), click on Prepare Addenda Measurement (Fig. 17) and follow the wizard installation instructions.

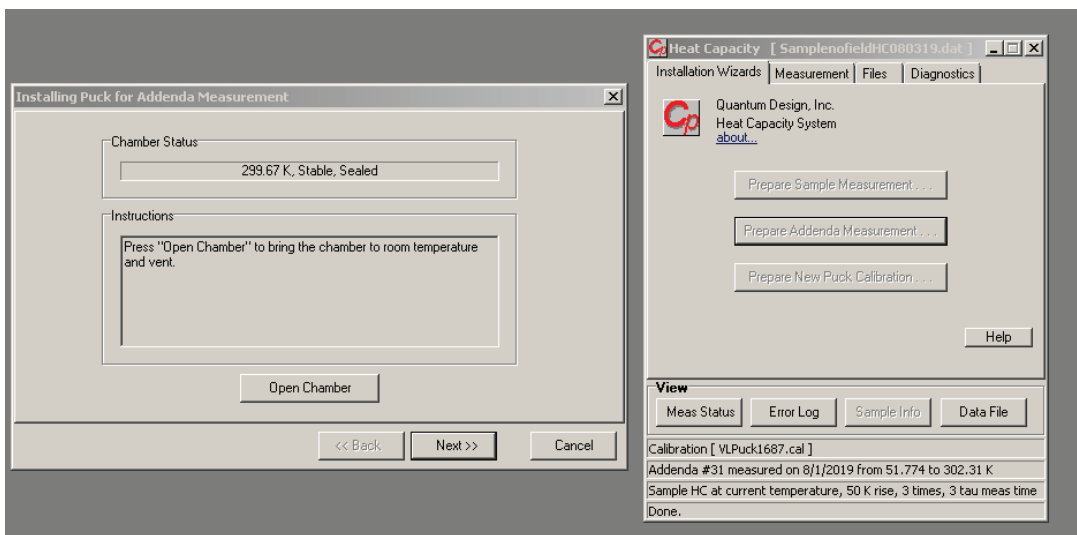


Figure 17: Preparing the addenda measurement.

- i.) Under the measurement tab, there is the option to create a new addenda table (Fig. 18). For these measurements, select the default settings, which covers the full range 50 K – 389 K. Note that only 20 points are required, as the grease and sample heat capacity can be very well fit to a smooth curve. The addenda measurement will take some time (potentially a few hours); at the end, it is appended to the calibration file that will be used for the subsequent sample measurements.

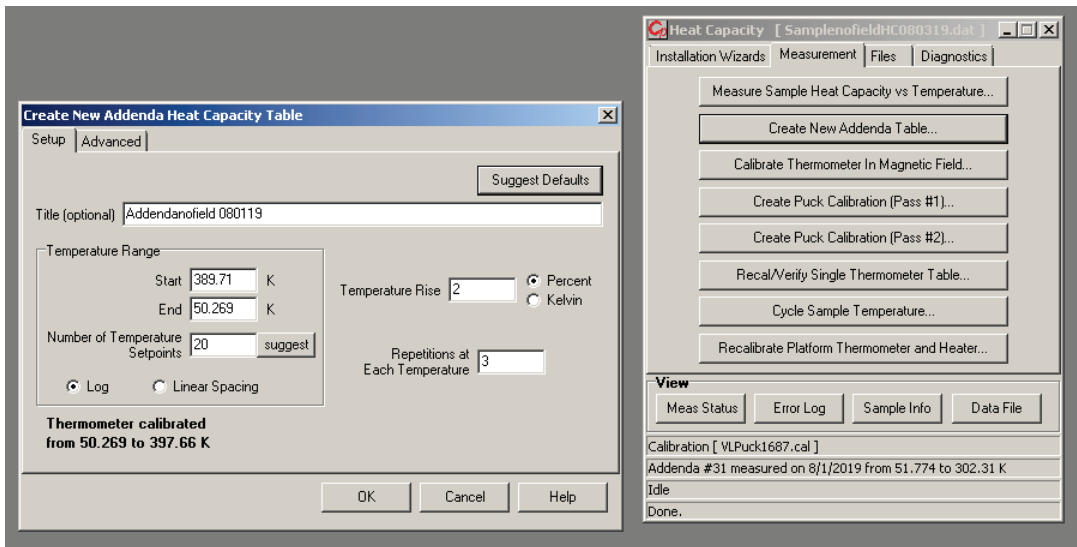


Figure 18: Configuring the addenda measurement.

- j.) After the addenda measurement is completed and the sample puck is at room temperature, it can be removed from the VersaLab in preparation for placing the sample onto the heat capacity platform.
- k.) The first step is to weigh a small piece of sample. Only a few mg are needed, so small, thin pieces are preferred to make sure there is good coupling with the measurement platform.
- l.) The heat capacity puck should be placed back in the mounting station to install the sample. This operation is often easier if the puck/station is under a microscope.
- m.) The sample should be gently placed onto the platform in the area where the N grease is located (Fig. 19). It is important to not remove any grease as this will invalidate the previously obtained addenda. Gently press down on the sample to ensure it is in close contact with the platform and not separated from it by a substantial amount of grease.

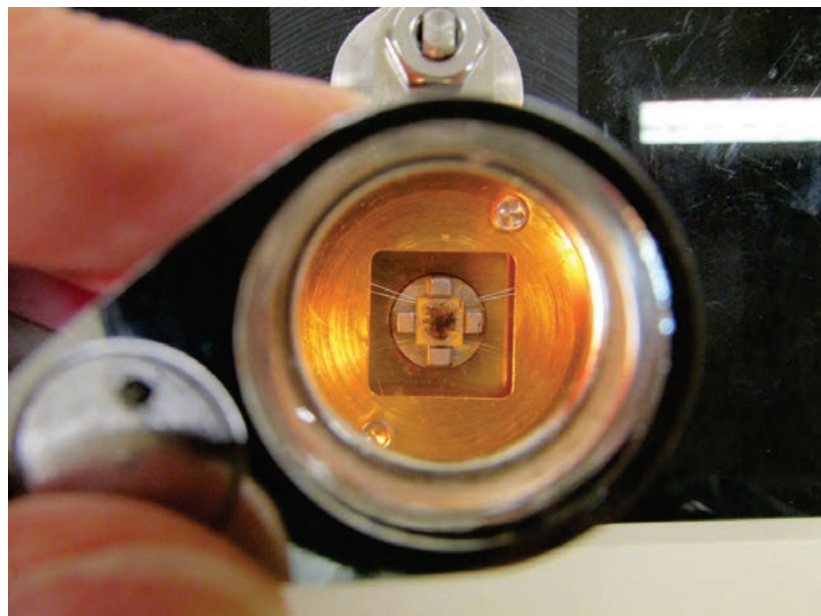


Figure 19: Heat capacity puck with sample deposited.

- n.) Remove the heat capacity puck, install the thermal shield (*i.e.* as in Fig. 14) and place it in the VersaLab to prepare for the heat capacity measurement.
- o.) After the sample is loaded, you are ready to perform the heat capacity measurement. Click on Prepare Sample Measurement and follow the wizard installation instructions (Fig. 20).

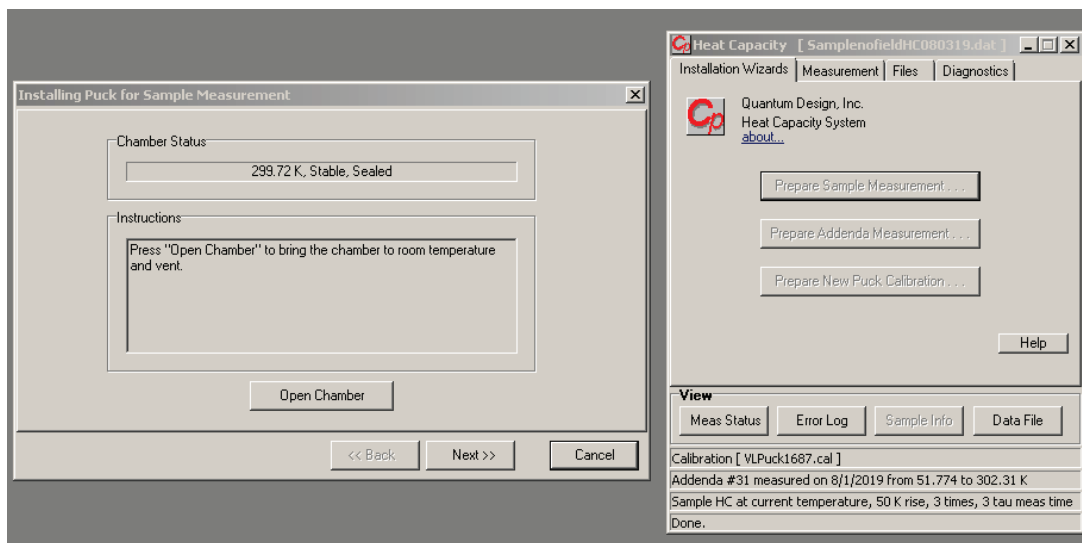


Figure 20: Preparing the sample measurement.

- p.) For now, the heat capacity will be measured from 50 K to 300 K to get a sense of the overall sample behavior. In the heat capacity control center, click on the measurement tab (Fig. 21). Click on Measure Sample Heat Capacity vs. Temperature. Click on suggest defaults, which will measure the sample heat capacity from 50 K – 300 K. Click OK. This will take several hours.

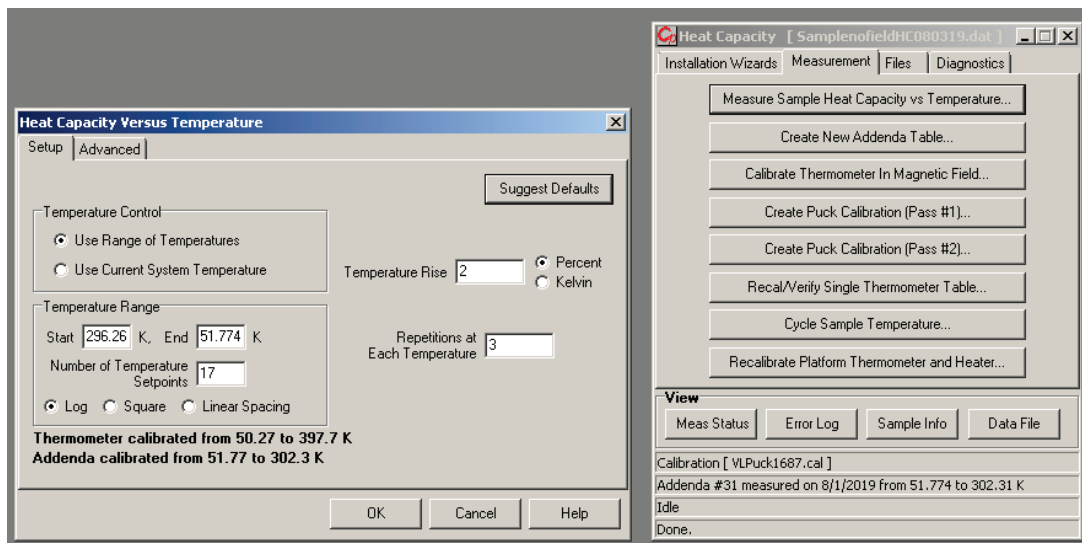


Figure 21: Measuring the sample.

- q.) The real time measurement status viewer should appear when the measurement starts (Fig. 22). Alternatively, on the Files tab, click on Measurement Status in order to bring it up. As the measurement progresses, expect the display to be similar to Fig. 5.

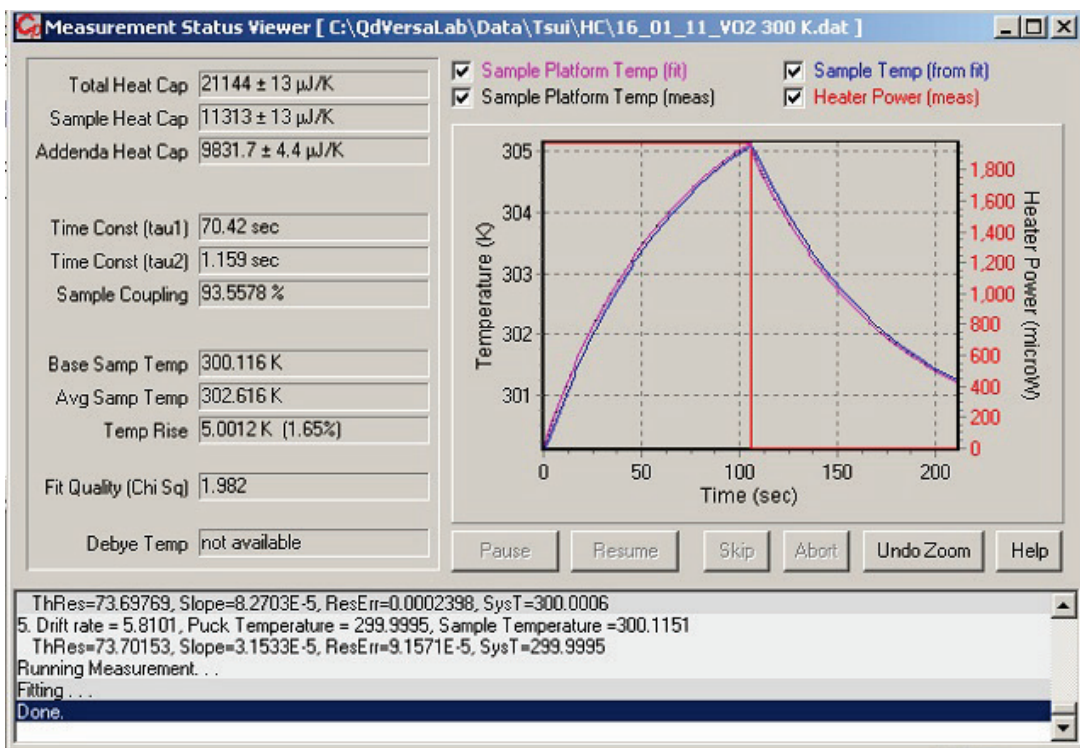


Figure 22: The measurement status viewer.

- r.) When your measurement is complete, go to the Files tab and click on Data File under the **View** section. How does your magnetite data compare to the diamond data in Fig. 4? Is there any indication of the Verwey transition in your data?
- s.) Next, the measurement is reconfigured to observe the Verwey transition using the slope analysis of relaxation curves to obtain the data. One approach is to write a simple sequence that will focus on measuring the heat capacity just about the transition:

```

Set Temperature 100K at 12K/min. Fast Settle
Wait For Temperature, Delay 300 secs, No Action
Sample HC at current temperature, 50 K rise, 3 times, 3 tau meas. time
Set Temperature 300K at 12K/min. Fast Settle

```

This sequence sets the initial temperature to 100 K, then performs a measurement three times, ramping the temperature up to 150 K (Fig. 23). Once the sequence is initiated, the measurement status viewer will appear on the screen to enable tracking of the measurement. A warning about inaccurate C_p values arising from this sequence may appear; this is given since the large temperature range covered which would lead to errors in a

conventional fitting with a 1-tau or 2-tau model. However, for the slope analysis method a sufficient temperature rise covering the first order phase transition is desired.

Alternatively, this measurement can be manually performed by setting the chamber temperature to 100 K, waiting for the temperature to stabilize, and use the Measure Sample Heat Capacity vs. Temperature function in the heat capacity control center.

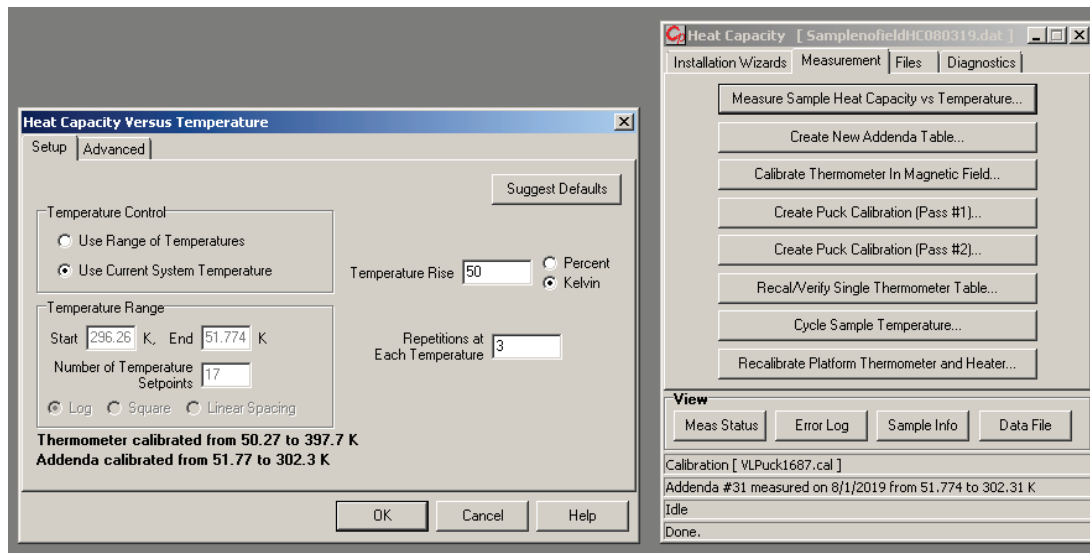


Figure 23: Measuring the sample using a single temperature rise for the slope analysis method.

- t.) The data can be analyzed within MultiVu. From the heat capacity control panel (Fig. 24, left side) under tab files, select "Raw Data File Viewing and Post Processing." A screen will appear as in Fig. 24 on the right.

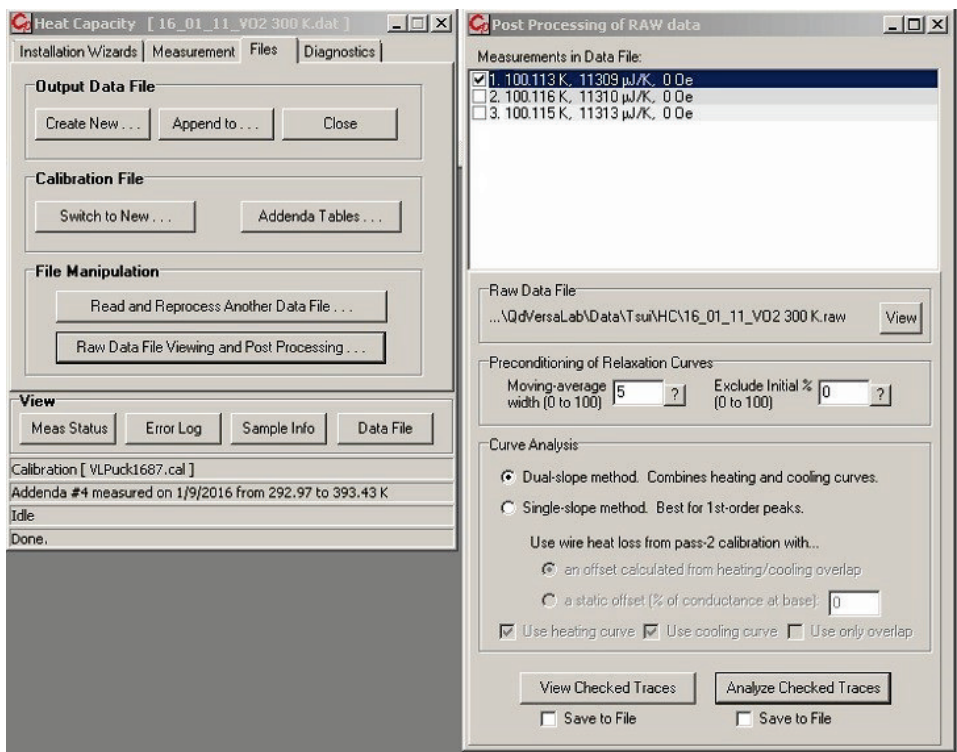


Figure 24: Screenshot of control panel and post processing window

- u.) Select the single slope curve analysis method appropriate for a first order phase transition. You can then view the checked traces (of which there are three as requested in the sequence), which will bring up a window of the raw data. Save this data to a file.
- v.) Now analyze the checked traces. Save this data to a file.

Discussion:

1. How does the data differ at temperatures away from the transition and at the transition? What do you notice in both the raw data and the checked traces?
2. Explain in more detail what the structural transition is for Fe_3O_4 at the Verwey temperature. How does it explain your results?
3. What is your Verwey transition temperature, and how do you know that you have identified the transition?
4. Analyze your data to estimate the mass specific heat below the transition temperature. Provide an estimate of the error bars and compare your result to experimentally published data for this material.

5. Analyze your data to obtain an estimate of the latent heat.
6. Plot the entropy S vs. temperature from your data. Think about what the change of entropy means. What would indicate a structural phase transition versus, for instance, a purely magnetic phase transition? Compare the change of entropy at the Verwey transition from your data to that expected of $S = k \ln \Omega$, where Ω is the multiplicity.

References:

- [1] A. Mills, "The lodestone: history, physics, and formation," *Annals of Science* 61, 273-319 (2003).
- [2] Alfa Aesar chemical supply. <https://www.alfa.com/en/catalog/012374/>
- [3] D.R. Lovley et al., "Anaerobic production of magnetite by a dissimilatory iron-reducing microorganism," *Nature* 330, 252-254 (1987).
- [4] E.J. Verwey, "Electronic conduction of magnetite (Fe_3O_4) and its transition point at low temperatures," *Nature* 144, 327-328 (1939).
- [5] S. Borroni et al., "On the Verwey transition in magnetite: the soft modes of the metal-insulator transition," <https://arxiv.org/pdf/1507.07193.pdf>.
- [6] M. Bohra et al., "Magnetic properties of magnetite thin films close to the Verwey transition," *Journal of Magnetism and Magnetic Materials* 321, 3738-3741 (2009).
- [7] G. Kh. Rozenberg et al., "Structural characterization of temperature- and pressure-induced inverse normal \leftrightarrow spinel transformation in magnetite," *Physical Review B* 75, 020102 (2007).
- [8] S. de Jong et al., "Speed limit of the insulator-metal transition in magnetite," *Nature Materials* 12, 882 (2013).
- [9] D. V. Schroeder, An Introduction to thermal physics, Addison Wesley, New York, 2000.
- [10] Steven H. Simon, The Oxford Solid State Basics, Oxford University Press, Oxford, 2013.
- [11] A. Einstein, Ann. Phys. 22, 180 (1907); see also any solid state physics book such as Simon's book in reference three.
- [12] https://en.wikipedia.org/wiki/Heavy_fermion
- [13] P. Coleman, Heavy Fermions: Electrons at the edge of magnetism, <https://arxiv.org/abs/cond-mat/0612006v3>
- [14] David L. Sidebottom, Fundamentals of Condensed Matter and Crystalline Physics, Cambridge University Press, Cambridge, 2012. Chapter 15.
- [15] D. I. Khomskii, Basics Aspects of the Quantum Theory of Solids, Order and Elementary Excitations, Cambridge University Press, Cambridge 2010.
- [16] P. M. Chaikin and T. C. Lubensky, Principles of Condensed Matter Physics, Cambridge University Press, Cambridge, 1995.